EUROPHYSICS LETTERS 1 January 1996

Europhys. Lett., **23** (1), pp. 1-5 (1993)

GROWTH AND SCALING IN ANISOTROPIC SPINODAL DECOMPOSITION

P. I. Hurtado[1], J. Marro[1], E. V. Albano[2]

[1] *Instituto* Carlos I *de Física Teórica y Computacional, and Departamento de Electromagnetismo y Física de la Materia, Universidad de Granada, 18071-Granada, Spain.*

[2] *Instituto de Investigaciones Fisicoquímicas Teóricas y Aplicadas, UNLP, CONICET, Sucursal 4, Casilla de Correo 16, (1900) La Plata, Argentina.*

(received ; accepted)

PACS. 05.20.Dd– Kinetic theory.
PACS. 61.20.Ja – Computer simulation of liquid structure.
PACS. 64.60.Qb– Nucleation.

Abstract. – We studied phase separation in a particle interacting system under a large drive along x. We here identify the basic growth mechanisms, and demonstrate time self-similarity, finite-size scaling, as well as other interesting features of both the structure factor and the scaling function. We also show that, at late t in two dimensions, there is a unique $t-$*dependent* length increasing $\ell_y(t) \sim t^{1/3}$ for macroscopic systems. Our results, which follow as a direct consequence of the underlying anisotropy, may characterize a class of nonequilibrium situations.

Many binary mixtures, e.g. the alloy Al-Zn, which are homogeneous at high temperature, develop coarsening macroscopic grains after a quench into the miscibility gap. The details of nucleation and spinodal decomposition as the system evolves towards coexistence of the two new phases determines various properties; e.g. hardness and resistivity of the alloy depend on how phase separation kinetics competes with the progress of solidification from the melt.

The involved essential physics is rather well understood, partly due to computer simulation of lattice gases.[1, 2] An interesting task is now understanding more general situations, e.g. lack of isotropy, which bears great technological importance. Mixtures under a shear flow attracted considerable attention as a possible scenario.[3]-[5] We studied the kinetics of the driven lattice gas (DLG) [6] by extensive Monte Carlo (MC) simulation. This is appealing on several grounds. Firstly, the DLG is the most successful, microscopic metaphor for (nonequilibrium) anisotropic phenomena, and its time relaxation remains intriguing.[7]-[11] Furthermore, the common underlying anisotropy might induce essential macroscopic similarities between the DLG and the sheared lattice gas,[4] as recent results on critical behavior seem to suggest.[12, 11] In any case, the DLG is not affected by hydrodynamic effects, which makes physics simpler.[1]

The DLG is a $d-$dimensional lattice gas (or, alternatively, binary alloy) at temperature T in which nearest-neighbor (NN) particle/hole exchanges are favored along one of the principal

lattice directions, say $\vec{x}$.[7] There are variables $n_i = 1$ (*particle*) or 0 (*hole*) at each site $i = 1, \ldots, N$, a NN interaction according to $H = -4 \sum_{NN} n_i n_j$, toroidal boundary conditions, and a transition rate given (e.g.) by a −biased− Metropolis algorithm, $\omega(\mathbf{n} \to \mathbf{n}^*) = \min\{1, \exp[-(\Delta H + E\delta)/T]\}$, which conserves density $\rho = N^{-1} \sum_i n_i$. Here, $\mathbf{n}^*$ represents configuration $\mathbf{n} = \{\mathbf{n_i}\}$ after jumping of a particle to a NN hole, $E\vec{x}$ may be interpreted as an (electric) field driving (charged) particles, $\Delta H = H(\mathbf{n}^*) - H(\mathbf{n})$, and $\delta = (\mp 1, 0)$ for jumps along $\pm\vec{x}$ or along any of the transverse directions, say $\vec{y}$, respectively.

The DLG was described as modelling fast ionic conduction, surface growth, traffic flow, etc.[7] A common feature of all these situations is anisotropy, and that steady states are out of equilibrium; both are essential features of the DLG induced by the rate ω. In general, ω violates detailed balance. This symmetry holds only for $E = 0$; the DLG then reduces to the familiar lattice gas with a unique (equilibrium) steady state independent of $\omega(\mathbf{n} \to \mathbf{n}^*)$. For any, even small E the steady state depends on ω, and a different, qualitatively new behavior emerges.[12] As E is increased, one eventually reaches saturation (particles cannot jump backwards, $-\vec{x}$), which is formally denoted as "$E = \infty$".

For $d = 2$, $\rho = \frac{1}{2}$ and $E = \infty$ (the only case to which we refer here for simplicity –also because this is a most interesting case [7]), a critical point occurs at $T = T_C^\infty \simeq 1.4 T_C\,(E = 0)$. Steady states below T_C^∞ do not correspond to coexistence of two thermodynamic (equilibrium) phases as for $E = 0$. Instead, stable ordered states consist of one single stripe, corresponding to the *liquid*, rich-particle phase, and *gas*, poor-particle phase filling the remainder of the system. The interface is linear and flat, except for microscopic roughness (which slightly increases with decreasing E). One measures a net current of particles along $\vec{x}$ (its intensity increasing with T, and changing slope at T_C^∞).[7]

Our simulations (fig.1) proceed by means of ω from a random state, until one or sometimes a few stripes are obtained. The code includes a list of $\lambda(t)$ particle-hole NN pairs from where the next move is drawn. Time is then increased by $\Delta t = \lambda(t)^{-1}$, so that its unit or *MC step* involves a visit to all sites on the average. Most evolutions are at $T = 0.8 T_C(E = 0) \simeq 0.6 T_C^\infty$ for which clustering is rather compact and, in practice, one can observe the full process of relaxation; we are assuming that, as observed for equilibrium states,[1]-[2] time evolution has the same properties in a wide region of the miscibility gap (see argument below). The lattice is rectangular, $L_x \times L_y$, with sides ranging from 64 to 256 (and, exceptionally, 512).

Starting from complete disorder, there is a very short regime in which small grains form (fig. 1a). Typical grains are anisotropic, stretched along $\vec{x}$. One then observes a rapid coarsening to form macroscopic strings, fig.1b. We skip details concerning such nucleation and early phase separation.[13] We wish to notice, however, that sheared fluids seem to depict a similar behavior. That is, initial formation of small anisotropic clusters (inducing a larger growth rate along the flow than in the other directions), and stringlike domains extending macroscopically have been reported in fluids.[3, 5]

After the initial (anisotropic) nucleation regime, strings coarsen further into well defined, relatively narrow stripes; fig.1c. The resulting multistripe states are not stable. They are partially segregated, and tend to relax towards the true stable state of one stripe. This may take a long macroscopic (say, *infinite*) time; in fact, the mean relaxation time increases with system size (see also [9]). As in the equilibrium case,[1] this is a consequence of the conservation of ρ, which makes the interfaces to depend on each other. It is true that certain individual runs sometimes block for a long time in a state with a few stripes; however, it does not seem to correspond to the average behavior. Typically, the number of stripes monotonically decreases with time, and the whole relaxation can easily be observed in computer simulations if one waits long enough (see caption for fig. 1).

We shall assume that further coarsening occurs by monomer diffusion. *Liquid* stripes

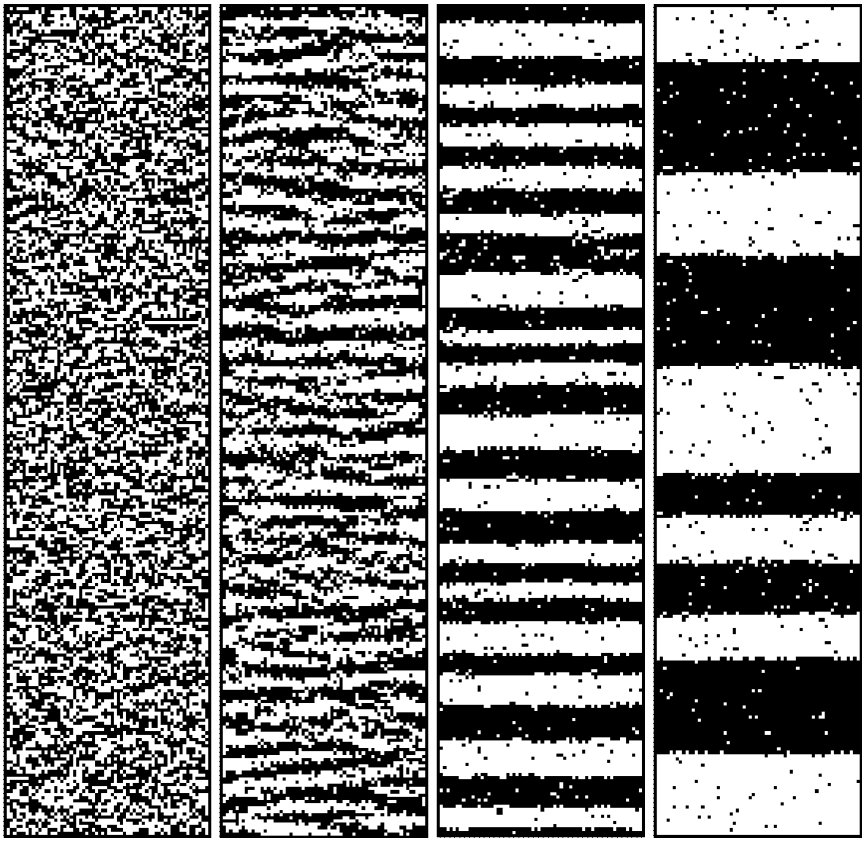

Fig. 1. – A series of snapshots depicting growth at $T \simeq 0.6T_C^\infty$ for $L_y \times L_x = 256 \times 64$ and $t = 1$ (a), 50 (b), 10^4 (c) and $2{\times}10^6$ (d) MC steps. In this particular run, two stripes were observed just before 10^7 MC steps while a single stripe was only reached after 10^8 MC steps.

thus effectively diffuse and, eventually, collide and coalesce with one neighbor. This implies evaporation of a *gas* stripe. Therefore, given the particle/hole symmetry, our assumption is equivalent −though it allows for a more detailed description below− to assuming coarsening by stripe evaporation as in [9].

Let us evaluate sort of *mobility* $\mathcal{D}_\ell$ due to stripe diffusion via monomer events. Here $\mathcal{D}_\ell$ is the mean squared displacement of the stripe's center of mass per unit time. Consider a compact stripe of mean width $\ell(t)$ consisting of $j = 1, \ldots, M$ particles at $y_j(t)$. Its center of mass is at $Y_{cm}(t) = M^{-1} \sum_j y_j(t)$. Then $\mathcal{D}_\ell = N_{me} \langle (\Delta Y_{cm})^2 \rangle$, with N_{me} the frequency of events and $\langle (\Delta Y_{cm})^2 \rangle$ the mean squared displacement associated with one of them.[10] It ensues $\mathcal{D}_\ell$ as the result of two competing processes:
(A) A surface traps a monomer evaporated from the same interface.[14] Then $N_{me,A} = \nu \sum_j' \exp(-2\beta\Delta_j)$ where ν is a frequency, the sum is over the surface particles, β is the inverse temperature and Δ_j is the number of broken bonds. For flat linear interfaces, $N_{me,A} \approx 4\nu L_x \exp(-2\beta\bar{\Delta})$ where $\bar{\Delta}$ is the mean of Δ_j (we here multiplied by 2 to account for evaporation of surface holes reaching the surface again from the interior). One further has $\Delta Y_{cm} = M^{-1}\delta y$, where δy is the net displacement, and (for compact enough stripes) $M \approx L_x \times \ell(t)$, so that $\langle (\Delta Y_{cm})^2 \rangle = \langle \delta y^2 \rangle \; L_x^{-2} \ell^{-2}$.

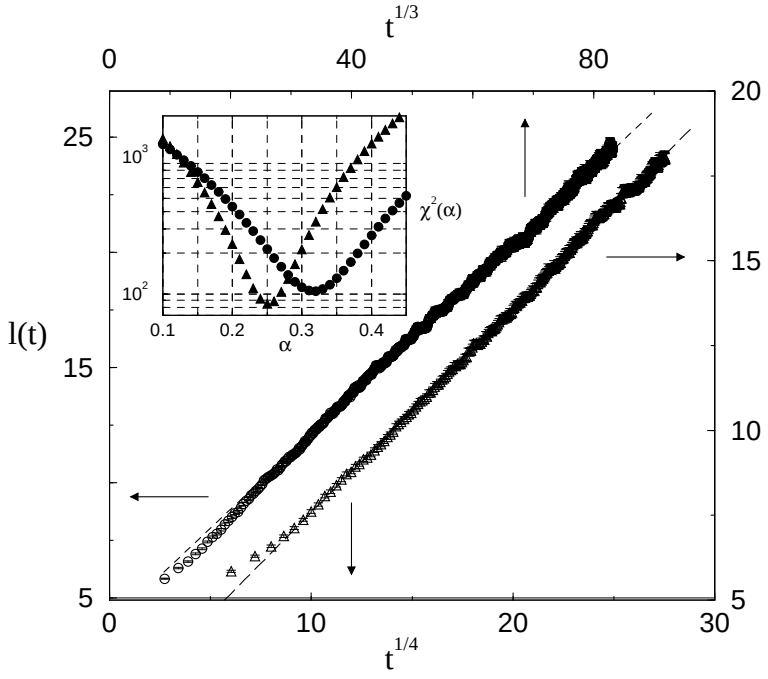

Fig. 2. – The typical length $\ell\,(t)$ versus t^{ϕ_y} for a lattice of size 64×64 (Δ), with $\phi_y = \frac{1}{4}$, and 256×64 (O), with $\phi_y = \frac{1}{3}$. (Note that each set of data refers to different axis.) The inset shows Pearson Chi Square function, $\chi^2\,(\phi_y)$, for varying fits.

(B) A hole jumps within the stripe, inducing $\Delta Y_{cm} = 1/M$ or 0 depending on the jump direction. One has $N_{me,B} = 2\nu\rho_h(T)L_x\ell p_h(T)$, where $\rho_h L_x \ell$ is the number of holes in the stripe and p_h is a jumping probability. At low T (small hole density ρ_h), holes are isolated from each other, so that $p_h \approx 1$. It ensues $\mathcal{D}_\ell^{(B)} \sim 2\nu\rho_h L_x^{-1}\ell^{-1}$.

As far as stripes are a distance ℓ apart from each other, they take a time $\tau_\ell = \ell^2/\mathcal{D}_\ell$ to meet, which increases width by ℓ. Then $d\ell/dt \sim \mathcal{D}_\ell\ell^{-1}$ and, assuming that processes A and B are independent,

$$d\ell/dt \sim L_x^{-1}(\alpha_A\ell^{-3} + \alpha_B\ell^{-2})$$

for low T and large E; here, $\alpha_A = 4\nu\langle\delta y^2\rangle e^{-2\beta\bar{\Delta}}$ and $\alpha_B = 2\nu\rho_h$.

This has some interesting implications. At late times, $\ell(t) \sim \alpha t^{1/3} + \alpha_A/2\alpha_B$ with $\alpha^3 = 3\alpha_B L_x^{-1}$, i.e., hole diffusion (mechanism B) is dominant. Evaporation/condensation (mechanism A) results in $t^{1/4}$ behavior; this is predicted to matter earlier. The crossover between the two mechanisms is for $t \sim \tau_{cross} = (4\alpha_A)^3(3\alpha_B)^{-4}L_x$, i.e., a macroscopic, observable time. If we define the time at which a single stripe forms, $\ell(\tau_{ss}) \approx \frac{1}{2}L_y$, it follows that the $t^{1/3}$ behavior is dominant for $\gamma(T, L_y, L_x) \equiv \tau_{cross}/\tau_{ss} \ll 1$. It also follows $\gamma \to 0$ for finite T in the thermodynamic limit. Consequently, our theory predicts that the $t^{1/3}$ growth is the general one to be observed, as it is also concluded in [9]; the $t^{1/4}$ growth should only be observable in "small" −as defined below− systems. It is to be noted that, in equilibrium, the Lifshitz-Slyozov-Wagner mechanism (evaporation from small grains of high curvature and, after diffusion, condensation onto larger grains) implies $\ell \sim t^{1/3}$, in accordance with experiments.

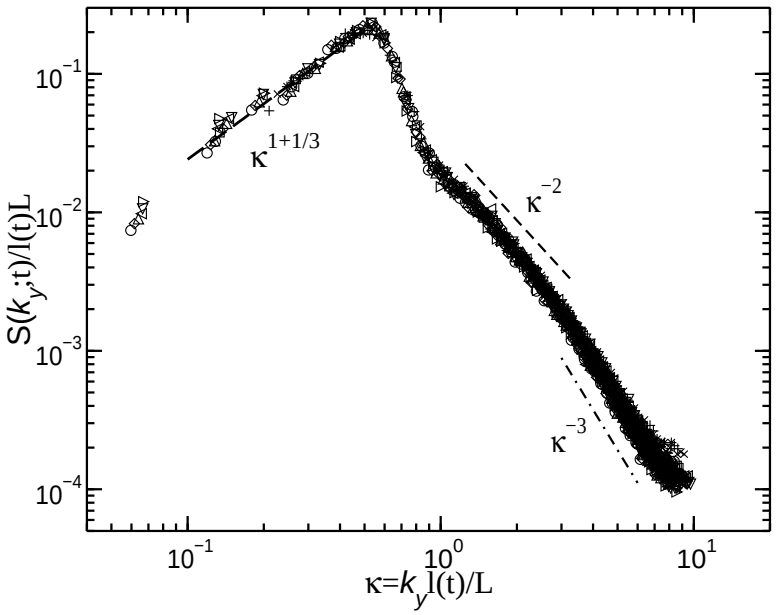

Fig. 3. – Scaling with size and time of the structure factor. The plot includes data from 64×64, 128×128 and 256×256 lattices, and times $t > 10^4$ MC steps. The relevant behaviors (see the main text) are indicated by dashed lines; $\kappa \equiv k_y \ell / L$.

Let us define a longitudinal length, $\ell_x \sim t^{\phi_x}$;[2, 9] one expects more rapid growth than transversely, $\phi_x > 1/3$. Concerning $t-$dependence, this length is only relevant initially, until well-defined stripes form. This interesting result concerns time dependence far from criticality. It is compatible with the possible existence of two *correlation* lengths near T_C^∞ which describe thermal fluctuations.[12] Note also that the onset of the multistripe state, when only $\ell_y(t)$ is relevant, may be defined by $\ell_x(\tau_{ms}) = L_x$, i.e., $\tau_{ms} \sim L_x^{1/\phi_x}$, which is on the same macroscopic time scale as τ_{cross} and τ_{ss}.

The structure factor is, setting $k_x = 0$ (the dependence on k_x is only relevant at early times):

$$S(k_y; t) = \frac{1}{L_x L_y} \left| \sum_{x,y} n_{x,y}(t) \exp[i k_y y] \right|^2 .$$

This soon develops a peak at $k_y = k_{max}(t)$ that shifts towards smaller wave number with increasing t. We define $\ell_S = 2\pi / k_{max}$ as a measure of the mean stripe width. Alternatively, one may use the first moment of S, or the slope of the straight portion in a plot of $\ln[S(k_y, t)]$ *versus* $(k_y - k_{max})^2$, which is known as *Guinier radius* . One may also monitor the number of stripes N_s and, averaging over all stripes in a given configuration, their maximum width, ℓ_{max} and $\ell_M \equiv M/L_x$. After performing an extra average over more than one thousand independent evolutions, all these quantities happen to exhibit essentially the same dependence on t; we denote $\ell(t)$ this common behavior.

To check our predictions, we plotted $\ell(t)$ versus t^{ϕ_y} for varying ϕ_y looking for the best linear fit. As illustrated in the inset of fig. 2, χ^2 associated with this fit nicely confirms that $\phi_y \simeq \frac{1}{4}$ for *small* systems ($L_y < 128$) while $\phi_y \simeq \frac{1}{3}$ for *large* ones ($L_y \geq 256$). This is further

confirmed by studying $d\ln\ell\ /d\ln t$ for large ℓ (not shown). Our theory predicts that this crossover with size will occur for $\tau_{cross} = \tau_{ss}$. For flat linear interfaces, $\langle \delta y^2 \rangle \sim \mathcal{O}(1)$, $\bar{\Delta} \leq 6$, $\rho_h \sim \exp(-16/T)$ and $\nu \simeq 1/q$, the lattice coordination number. It then follows numerically that the crossover from the early $\phi_y = \frac{1}{4}$ to the general macroscopic $\frac{1}{3}$ behavior will occur around $L_y \sim 140$ for $L_x = 64$. Again, this is fully consistent with our observations. The reason behind is that surfaces (and, thus, mechanism A) dominate initially, more the smaller the system is; however, hole diffusion (B) tends to dominate as the system relaxes towards only two surfaces enclosing the whole of the liquid phase.

The structure factor is an important tool for experimental analysis. Given that the DLG shows a unique t-dependent length after forming stripes, one should expect $S(k_y;t) \propto \ell(t)F[k_y\ell(t)]$. This is confirmed in fig. 3. (A Ginzburg-Landau model for sheared mixtures has been shown to exhibit a similar property, though with two lengths both behaving differently than $\ell(t)$ here.[5]) Fig. 3 also illustrates that data for different square lattices scale $S\ell^{-1}L^{-1} \sim F(\eta L^{-1})$, $\eta \equiv k_y\ell$. A similar result does not hold for general, rectangular lattices, as one should probably expect due to more involved finite-size effects if $L_x \neq L_y$.

The sphericallized function for a three-dimensional system relaxing to equilibrium was shown to satisfy $S(k,t) = J(t) \cdot F[kR(t)]$. This turned out most useful given that R and J can simply be evaluated phenomenologically as the scaling lengths for the k and S axes, respectively. In particular, it then followed $F(\eta) = \Phi(\eta) \cdot \Psi[\eta \cdot \sigma(\rho, T)]$, with Φ and Ψ universal functions. Φ describes the diffraction by a single grain, Ψ is a *grain interference function*, and σ characterizes the point in the phase diagram where the sample is quenched. In this way, it was shown [2] that $\Psi \approx 1$ except at small values of k, so that, for large η, $F(\eta)$ becomes independent of T, ρ, and even the substance investigated. Though we only obtained some weak, indirect evidence of this for the DLG (which was investigated systematically for just one phase point), it suggests that assuming a wide range of validity of our conclusions here is sensible.

In equilibrium, $\Phi(\eta)$ is predicted to decay according to Porod law,[1] η^{-3} (for $d = 2$) at large η. In the DLG, this concerns the region $\xi_y \ll k_y^{-1} \ll \ell(t)$, where ξ_y is the transverse correlation length, and the striped geometry implies a two-point correlation function $C_t(x,t) \sim \frac{1}{2}(1 - x\ell^{-1})$, $x \ll \ell$. Therefore, we predict that $\Phi \sim \eta^{-2}$ is the characteristic anisotropic behavior corresponding to Porod law. This is confirmed in fig. 3. Interesting enough, this property of the scaling function implies $S \sim 1/\ell\,(t)\,k_y^2$ for k_y larger than for the Guinier gaussian region described above. Finally, we remark that the behavior $\Phi \sim \eta^{-2}$ is general except (for *large* systems) at large enough values of η (fig. 3). In this case, the standard Porod law holds, which is induced by the very small, standard thermal clustering (which is here similar to the one in equilibrium).

Summing up, we showed time self-similarity and simple finite-size scaling of the structure factor in a (nonequilibrium) particle model under a large drive following a quench to low T. In spite of some formal similarities, both the scaling function and the structure factor differ from the ones for the equilibrium (not driven) case. This is a consequence of the singular geometry (flat linear interfaces) induced by the drive. The scaling function $\Phi(\eta)$ is seen to tend to an envelope $\sim \eta^{1+1/3}$ at small η; it then follows a gaussian peak $\sim exp[-const \cdot (\eta - \eta_{max})^2]$, and decays η^{-2} and, finally, η^{-3} at large η. On the other hand, there is only one $t-dependent$ relevant length, the mean interfaces distance. This generally grows as $t^{1/3}$ due to hole diffusion in the bulk, though one may also observe $t^{1/4}$ at very early times due to surface evaporation-condensation processes. The basic mechanisms are here much simpler than in equilibrium, again due to the underlying anisotropy. That is, the standard lattice gas typically develops grains of different sizes, showing a distribution from microscopic to macroscopic grains. This is the case for practically any t and, as a consequence, a detailed surface-tension-controlled

kinetic description is rather complex.[15] The DLG grain distribution, after a short transient time, exhibits a gap (at the, say, mesoscopic scale) between monomers and *infinite* grains, namely, stripes of varying width. Some of the DLG properties described here might hold in several other anisotropic situations. We hope related experiments will be performed that will motivate development of more complete theories.

Acknowledgments – We acknowledge useful discussions with P.L. Garrido, R. Monetti, M.A. Muñoz, L. Rubio and G. Saracco, and support from MCYT, projects PB97-0842 and BFM2001-2841.

REFERENCES

[1] For reviews, see K. Binder *et al*, *Adv. Colloid. Interf. Sci.*, **10** 173 (1979); J.D. Gunton *et al*, in *Phase Transitions and Critical Phenomena, Academic Press, N.Y.*, 1983; A.J. Bray, *Adv. Phys.*, **43** 357 (1994).

[2] J. Marro *et al*, *Phys. Rev. B*, **12** 2000 (1975); ibid, *Phys. Rev. Lett.*, **43** 282 (1979); P. Fratzl *et al*, *Acta metall.*, **31** 1849 (1983)

[3] A. Onuki, *J. Phys. Condens. Matter*, **9** 6119 (1997); N. Rapapa and A. Bray, *Phys. Rev. Lett.*, **83** 3856 (1999)

[4] C. Chan and L. Lin, *Europhys. Lett.*, **11** 13 (1990).

[5] F. Corberi *et al*, *Phys. Rev. E*, **61** 6621 (2000).

[6] S. Katz *et al*, *J. Stat. Phys.*, **34** 497 (1984).

[7] J. Marro and R. Dickman, *Nonequilibrium Phase Transitions in Lattice Models, Cambridge University Press, Cambridge, U.K.*, 1999.

[8] C. Yeung *et al.*, *J. Stat. Phys.*, **66** 1071 (1992); S. Puri *et al*, *J. Stat. Phys.*, **75** 839 (1994); F. Alexander *et al.*, *J. Stat. Phys.*, **82** 1133 (1996).

[9] E. Levine *et al*, *Phys. Rev. E*, **64** 26105 (2001).

[10] K. Binder, *Phys. Rev. B*, **15** 4425 (1977).

[11] E.V. Albano and G. Saracco, *preprint,*.

[12] A. Achahbar *et al.*, *Phys. Rev. Lett.*, **87** 195702 (2001).

[13] This initial regime of nucleation is theoretically more involved, e.g., one cannot assume flat linear interfaces (as we do below) and surface tension may play an important role. However, nucleation extends very shortly after the melt, thus bearing relatively less practical importance; cf. fig 1 and its caption.

[14] N.T.J. Bailey, *The Elements of Stochastic Processes, John Wiley & Sons, N.Y.*, 1964.

[15] O. Penrose *et al*, *J. Stat. Phys.*, **19** 243 (1978); ibid **34** 399 (1984)